Graded-index magnonics

C.S. Davies and V.V. Kruglyak

School of Physics, University of Exeter, Stocker road, Exeter EX4 4QL, United Kingdom
E-mail: V.V.Kruglyak@exeter.ac.uk

The wave solutions of the Landau–Lifshitz equation (spin waves) are characterized by some of the most complex and peculiar dispersion relations among all waves. For example, the spin-wave ("magnonic") dispersion can range from the parabolic law (typical for a quantum-mechanical electron) at short wavelengths to the nonanalytical linear type (typical for light and acoustic phonons) at long wavelengths. Moreover, the long-wavelength magnonic dispersion has a gap and is inherently anisotropic, being naturally negative for a range of relative orientations between the effective field and the spin-wave vector. Nonuniformities in the effective field and magnetization configurations enable the guiding and steering of spin waves in a deliberate manner and therefore represent landscapes of graded refractive index (graded magnonic index). By analogy to the fields of graded-index photonics and transformation optics, the studies of spin waves in graded magnonic landscapes can be united under the umbrella of the graded-index magnonics theme and are reviewed here with focus on the challenges and opportunities ahead of this exciting research direction.

1. Introduction

It can be somewhat surprising to recognize that the entire field of magnonics [1] – the study of spin waves [2,3] is built upon the foundation of the Landau–Lifshitz equation. [4] In an ordered ensemble of spins, immediate (and sometimes also somewhat more distant) neighbours are coupled via the quantum-mechanical exchange interaction, while the interaction between spins at further distances from each other is dominated by the magneto-dipole field, described by the Maxwell equations. By perturbing the static configuration of spins locally, propagating spin waves can be excited. The Landau–Lifshitz and Maxwell equations operate with the classical magnetization vector (**M**) defined as the average magnetic moment (associated with the spins) per unit volume. In this approximation, the spin waves take the form of propagating waves of precessing magnetization, and the Landau–Lifshitz equation relates the precession of the magnetization to the effective magnetic field, which can also be a function of the magnetization distribution in the sample.

Until recently, the majority of studies in magnonics dealt with samples either having or assuming uniform configurations (henceforth, we often refer to these as "landscapes") of the magnetization and magnetic field. This simplicity enabled detailed studies of the spin-wave ("magnonic") dispersion and the spectrum of standing spin waves, which have their wave vector quantized due to confinement by the geometrical boundaries of the sample. It has been established that the magnonic dispersion is intrinsically anisotropic in the dipole and dipole-exchange (i.e. long-wavelength) regimes but is isotropic in the exchange (short-wavelength) regime. In particular, the anisotropy of the magnonic dispersion can lead to extremely peculiar character of spin-wave propagation and scattering from geometrical boundaries [5–9]. Nonetheless, the direction of the spin-wave beam remains constant as long as the magnetic landscape remains uniform.

However, it was soon realized and increasingly often exploited that, by deforming the magnetic landscape via making either the magnetization or the effective magnetic field or both non-uniform, the propagation path of spin waves could be deliberately modified. The study of spin waves in continuously varying magnetic landscapes forms the scope and definition of the field of graded-index magnonics [10]. This is similar in spirit to (and indeed, has been inspired by) graded-index optics [11] (or transformation optics [12]), which seek to modify the light dispersion in photonic and electromagnetic systems using a spa-

tially varying ("graded") refractive index. However, the magnonic dispersion described by the Landau–Lifshitz equation is arguably far more complex and peculiar as compared to that of light, thereby offering extremely rich opportunities and a bright outlook to the field of graded-index magnonics. The field of magnonics has received a tremendous amount of attention in recent years, particularly due to the potential for spin waves to act as information carriers within the data storage, communication and processing technologies [13]. It is therefore perceived that graded-index magnonics as a theme may well simplify the construction of, and indeed give rise to, many technological applications just as transformation optics has done for electromagnetic technologies.

Here, we present a nonexhaustive review of the concept of the graded-index magnonics together with the key research results and directions that are united by this theme. We begin by briefly reminding the reader of the key equations governing the dispersion of spin waves in uniform media and their scattering from magnetic non-uniformities. The path of spin-wave beams through landscapes with a continuous variation of parameters that determine magnonic dispersion is then postulated to be a result of multiple scattering events from infinitesimally weak non-uniformities [14–16]. This idea is fed into the following review and discussion of a representative selection of studies of spin waves in nonuniform magnonic landscapes, which aim to show the diversity of phenomena falling under the markedly broad umbrella of the graded-index magnonics concept. The discussion is illustrated using numerical solutions of the Landau–Lifshitz equation (micromagnetic simulations [17,18]) obtained using Object-Oriented Micro-Magnetic Framework [19]. The paper is concluded with some general remarks on further progress in the field, with emphasis on opportunities arising from mapping ideas and methodology from transformation optics onto the exceptionally rich world of the Landau–Lifshitz equation and its solutions for graded-index magnonic media and devices.

2. Dispersion, propagation and scattering of spin waves in uniform thin magnetic films

As for any waves, the direction of the spin-wave propagation is given by the group velocity (v_g), calculated as the gradient of the frequency ($\omega = 2\pi f$) in the reciprocal space. The group-velocity vector is therefore orthogonal to curves of constant frequency, often referred to as isofrequency curves (or surfaces in the 3D case) [14]. Hence, we begin by reviewing the key results concerning the magnonic dispersion in thin-film magnetic samples.

The exchange interaction makes a negligible contribution to the dispersion of long-wavelength spin waves, which are therefore termed "magnetostatic" or "dipolar" waves. Their dispersion is implicitly defined by [20,21]

$$(\mu+1)k_z^2 + (\mu^2 - v^2 + 1)k_y^2 +$$

$$+ 2\mu\sqrt{k^2\left(-\frac{k_z^2}{\mu} - k_y^2\right)}\cot\left(s\sqrt{-\frac{k_z^2}{\mu} - k_y^2}\right) = 0 \quad (1)$$

where s is the film thickness, k_y and k_z are the in-plane projections of the wave vector with length k, and μ and v are

$$\mu = 1 + \frac{\omega_M \omega_H}{\omega_H^2 - \omega^2} \quad \text{and} \quad v = \frac{\omega_M \omega}{\omega_H^2 - \omega^2} \quad (2)$$

where $\omega_M = 4\pi\gamma M_S$, $\omega_H = \gamma H_i$, where H_i is the internal static magnetic field aligned along the z-axis, M_S is the magnetization of saturation and γ is the gyromagnetic ratio.

For each specific frequency value, Eq. (1) describes an isofrequency curve, every point of which corresponds to the wave vector of a spin wave that is allowed to propagate at this frequency. Fig. 1(a) shows two typical isofrequency curves for dipolar spin waves in a 7.5 μm thick thin film of yttrium–iron–garnet (YIG), assuming $H_i = 1.25$ kOe and $M_S = 139$ G. It is easy to see that generally the direction of the group velocity (normal to the curve) is not collinear with that of the wave vector, which is a direct consequence of the anisotropy of the dispersion relation. One of the two symmetry axes of the isofrequency curves is parallel to the magnetization. If ω is greater (smaller) than the frequency of the uniform ferromagnetic resonance $\omega_{FMR} = \sqrt{\omega_H(\omega_H + \omega_M)}$, the projection of the group velocity onto the direction of the wave vector is positive (negative).

As the spin-wave wavelength gets shorter, the exchange interaction cannot be neglected anymore and needs to be taken into account on equal footing with the magneto-dipole interaction. The dispersion of such so-called "dipole-exchange" spin waves can be written as [22]

$$\omega = \sqrt{(\omega_H + \gamma Dk^2)(\omega_H + \gamma Dk^2 + \omega_M F_{00})}, \quad (3)$$

where $D = 2A/M_S$ is the exchange stiffness (A is the exchange constant) and the zeroth dipole-dipole matrix element F_{00} is defined as

$$F_{00} = 1 + P_{00}\left[1 - P_{00}\left(\frac{\omega_M}{\omega_H + \gamma Dk^2}\right)\left(\frac{k_z}{k}\right)^2 - \left(\frac{k_y}{k}\right)^2\right]$$

$$\text{and} \quad P_{00} = 1 + \frac{1 - \exp(-ks)}{ks}.$$

Typical dipole-exchange isofrequency curves are shown in Fig. 1(b) for a 100 nm thick Permalloy [23] thin film, biased by $H_i = 500$ Oe. As the frequency of the dipole-exchange spin wave increases, the anisotropy of the dispersion decreases. At very short wavelength (and therefore very high frequencies), the isotropic exchange interaction
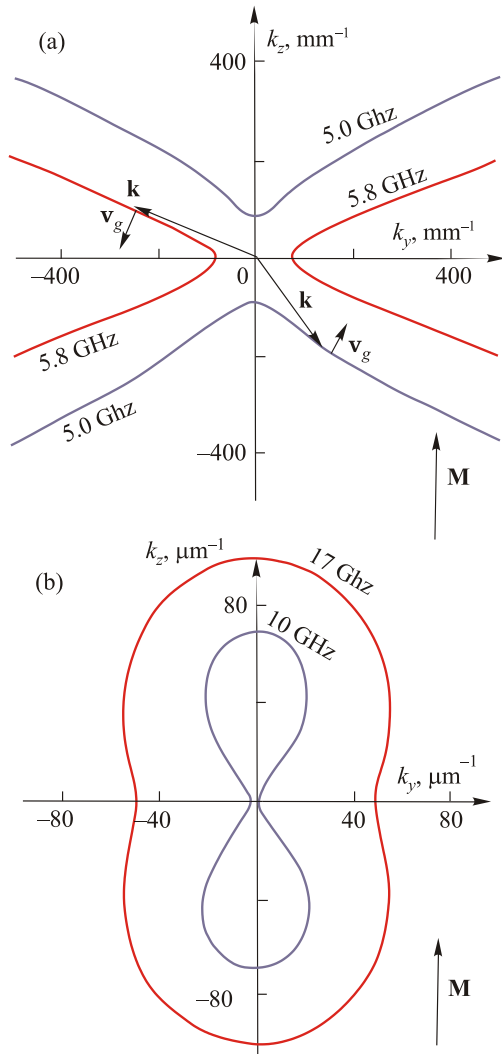
Fig. 1. (a) (Color online) Typical isofrequency curves of magnetostatic spin waves in a YIG film are plotted using Eqs. (1) and (2) for frequencies above (5.8 GHz) and below (5 GHz) the FMR frequency. Examples of group velocities v_g corresponding to wave vectors **k** are indicated schematically on each curve. (b) Typical isofrequency curves of dipole-exchange spin waves in a Permalloy thin film are plotted using Eq. (3) for frequencies of 10 GHz and 17 GHz.

dominates the magnonic dispersion. The dispersion of exchange spin waves is isotropic, and so, the corresponding isofrequency curves have circular shape.

The isofrequency curves presented in Fig. 1 are sufficient on their own to describe the propagation of spin waves across uniformly-magnetized media, e.g. to explain the origin of spin wave caustics [9,24]. Spin waves excited by a nearly point-like magnonic source [9,25,26] have a broad distribution of wave vectors. However, as can be seen from Fig. 1, significant sections of the magnetostatic isofrequency curves are nearly straight. Hence, whilst spin waves with a range of wave vectors are excited, their group velocities associated with these wave vectors tend to have similar, nearly collinear directions, leading to the for-

mation of tightly focused, narrow spin-wave caustic beams. In context of the perceived magnonic technology, it is important to note that the noncollinearity of the magnonic phase and group velocities within the beams represents a complication for designs of magnonic devices exploiting spin-wave phase [1,27–29].

The scattering (i.e. reflection and refraction) of spin waves from an interface between two uniform magnetic media [30] can also be described using the isofrequency-curve method. Let us first consider a magnonic caustic beam propagating across a uniform 7.5 μm thick YIG film biased by a magnetic field of non-uniform strength. For simplicity, we will assume that the field is parallel to the z-axis but its strength takes different values in and then remains constant within each of regions A, B and C of the sample (Fig. 2 (a)), so that $H_{i,A} = H_{i,C} = 11.7$ kOe $< H_{i,B} = 12$ kOe. Spin waves with frequency of 34.8 GHz and a broad distribution of wave vectors are excited by a dynamic field localized at the bottom left corner of the sample. As the spin wave beam propagates from Region A to B, it refracts away from the normal to the interface and then again refracts towards the normal as it propagates from Regions B to C (Fig. 2 (a)).The reflections of the beam from each interface and edge of the sample are also visible, albeit with a reduced intensity.

To understand the behavior observed in Fig. 2(a), the isofrequency curves belonging to each region of the sample are plotted in Fig. 2(b). Upon increasing the effective field strength (while keeping the frequency and the magnetization orientation fixed), the magnetostatic isofrequency curves on either side of the k_y-axis are pushed away from each other, leading to an increased gradient along their quasi-linear sections. We note that this behavior occurs only for
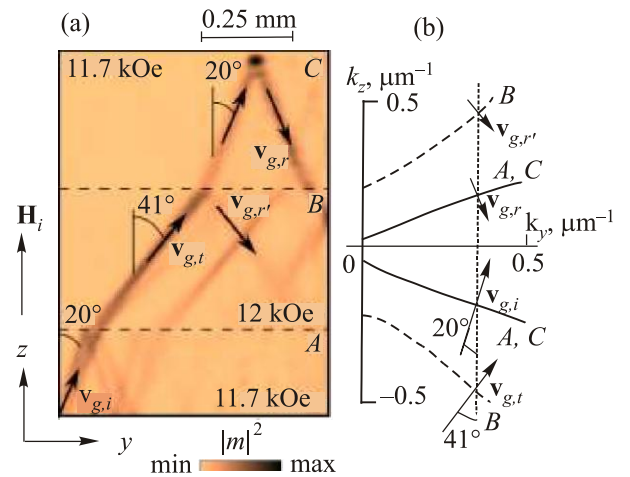

Fig. 2. (a) (Color online) The calculated distribution of the dynamic magnetization is shown for a spin wave excited at 34.82 GHz in the bottom left corner of the YIG sample. The arrows show the group velocity directions of the incident ($\mathbf{v}_{g,i}$), transmitted ($\mathbf{v}_{g,t}$) and reflected ($\mathbf{v}_{g,r}$) beams. (b) The isofrequency curves calculated for regions A and C (solid), and B (dashed) are shown for the spin-wave in panel (a).

$\omega < \omega_{FMR}$, as in the present case, but is reversed otherwise. The incident spin waves in Region *A* have a range of wave vector values and directions, even though the associated group velocities are nearly collinear (as explained earlier). Let us fix the wave-vector component that is parallel to the interface, i.e. k_y. The beam directions in the different regions of the sample will then be given by the normal to the isofrequency curves at points of their intersection by a vertical line corresponding to the selected k_y value.

The concept presented in Fig. 2 is the cornerstone of interpretation of many experimental observations in the field of graded-index magnonics. Moreover, by tracing the spatial evolution of isofrequency curves in media with continuous variation of magnetic properties defining the magnonic dispersion, one is able to not only explain but also predict and design the character of propagation and scattering of spin-wave beams. In the following, we review some of the most remarkable effects already observed in graded-index magnonic media (the properties of which are described by the Landau–Lifshitz equation) and furthermore consider the potential new avenues of research available to future researchers within this theme.

3. Brief review of effects observed in graded-index magnonic media

Perhaps, one of the first graded-index effects observed during the latest boom of magnonics research was the discovery of spin-wave modes confined within so-called "spin-wave wells", first in stripes [31,32] and then in squares and rectangles [33,34]. This confinement is a direct consequence of the existence in the magnonic dispersion of a threshold frequency below which spin waves cannot propagate or be excited. This threshold frequency approximately scales with the value of the static internal magnetic field. Hence, spin waves that are allowed in the regions of a reduced internal magnetic field (typically, created by the demagnetising field in magnetic elements of nonellipsoidal shape due to edge magnetic charges) are not allowed to propagate into the bulk of the sample, where the demagnetising field is reduced and the internal field is therefore increased.

This phenomenon of spin-wave confinement in internal magnetic field landscapes is analogous to confinement of a quantum-mechanical electron in a potential well, whereby the spin wave plays the role of the electron wave function and the internal magnetic field plays the role of the electron potential energy. However, the vectorial nature of the magnetic field makes it challenging to induce confinement in more than one dimension. Hence, a suitably excited spin wave could still propagate in the direction orthogonal to the direction of the field induced confinement, leading to the idea of spin-wave channeling [35,36]. The lateral extent of such magnonic channels (typically created close and parallel to the edge of a thin-film sample) is directly linked to the spin-wave frequency [37]. Moreover, by continuously varying the geometry of the magnonic waveguide and therefore of the associated non-uniform field distribution, the spin-wave channels can 'cling' to the edges of a nonrectangular structure, resulting in spin-wave splitting and potentially magnonic interferometer functionality [38].

The anisotropic dispersion of long-wavelength spin waves yields another (and probably, unique to magnonics) scheme of wave confinement. Indeed, by fixing the direction of the wave vector, we see from Fig. 1(a) that there exists a range of small *k*-values for which spin wave excitation is allowed for one but is forbidden for the other (orthogonal) direction of the magnetization relative to that of the wave vector. Hence, regions of curved magnetization can also prohibit propagation and therefore confine magnetostatic and dipole-exchange spin waves, as indeed was observed e.g. in Refs. 39,40. The same mechanism could lead to the confinement of spin waves in the in-plane direction that is orthogonal to that of the static internal magnetic field, e.g. when it is orthogonal to the edge of a thin-film magnetic stripe.

The variation of the internal magnetic field has also been used to continuously tune the wavelength of propagating spin waves. Let us consider the funnel-shaped Permalloy element shown in Fig. 3(a). With a transverse bias field applied ($H_B = 1.25$ kOe), the average demagnetizing field increases in strength as we move along the funnel from left to right [41]. As a result, the projection of the total internal field onto the magnetization decreases, thereby decreasing
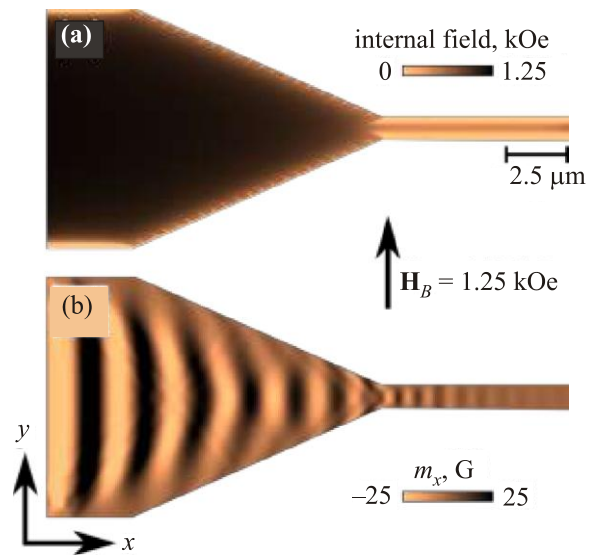

internal field, kOe

0 ▭▬ 1.25

2.5 μm

$\mathbf{H}_B = 1.25$ kOe

m_x, G

−25 ▭▬ 25

Fig. 3. (a) (Color online) The projection of the effective field on the static magnetization is shown for a 100 nm thick funnel-shaped Permalloy waveguide. (b) A snapshot of the out-of-plane component of the dynamic magnetization is shown for a spin wave excited harmonically at 14 GHz at the far left end of the waveguide.

also the spin-wave frequency at a given wavelength. Considering instead a fixed frequency, the vertices of the higher-frequency isofrequency curves in Fig. 1(a) move to higher k_y-values, and so, the spin-wave wavelength decreases. This wavelength reduction is clearly seen in the shown snapshot of the dynamic magnetization associated with the spin wave continuously excited at 14 GHz at the far left of the structure (Fig. 3(b)). It is interesting to note that the demonstration of this effect for a bulk YIG sample by Schlömann in 1964 was probably the first-ever manifestation of the graded-index magnonics principles discussed in literature [42]. The use of this so-called Schlömann mechanism of spin-wave excitation to couple free-space microwaves to spin waves of many orders of magnitude shorter wavelength propagating in Permalloy microstructures was demonstrated in Refs. 43,44. The formation of spin-wave wells discussed earlier can be interpreted as a result of the inability of the wavelength variation (at constant frequency) to compensate for the variation of the internal magnetic field.

In two dimensions, the spatial variation of the internal magnetic field and magnetization enables the steering of spin waves both in continuous films and networks of magnonic waveguides. The possibility of steering spin-wave caustics in thin magnetic films arises directly from the strict relationship between the directions of the static magnetization and caustics at a given value of the internal magnetic field. However, the continuous variation of the internal magnetic field and magnetization can lead to even more striking consequences, such as a complete disappearance of one of the spin-wave beams launched into a *T*-junction of magnonic wave guides [10]. Fig. 4(a) shows the configuration of the internal magnetic field and magnetization in an asymmetrically magnetized *T*-junction of 5 µm wide/100 nm thick Permalloy waveguides. Fig. 4(b) and (c) show snapshots of the dynamic magnetization due to a spin-wave beam propagating from the vertical "leg" into the right "arm" of the junction from time-resolved scanning Kerr microscopy (TRSKM) and OOMMF simulations, respectively. The spin-wave beam that was supposed to propagate to the left arm of the junction is absent, because the non-uniform field and magnetization (i.e. the "graded magnonic index") steer it into the lower edge of the left arm, from which it is then backward-reflected into the right arm of the junction. The curves and arrows in Fig. 4 (c) show the direction of the group velocity of the incident and reflected spin waves calculated using the approach presented in Fig. 2 (b). Of a special note is the curving of the spin-wave beam towards the normal to the rear edge of the arm by the graded magnonic index. This beam curving is a spin-wave analogue of the so-called "mirage effect", which was also observed in simulations from Ref. 45.

Even relatively small regions of graded magnonic index could either present obstacles for or find application in magnonic data and signal processing devices [46]. Indeed, any bending of magnonic waveguides necessarily leads either to spatial variation of the angle between the static
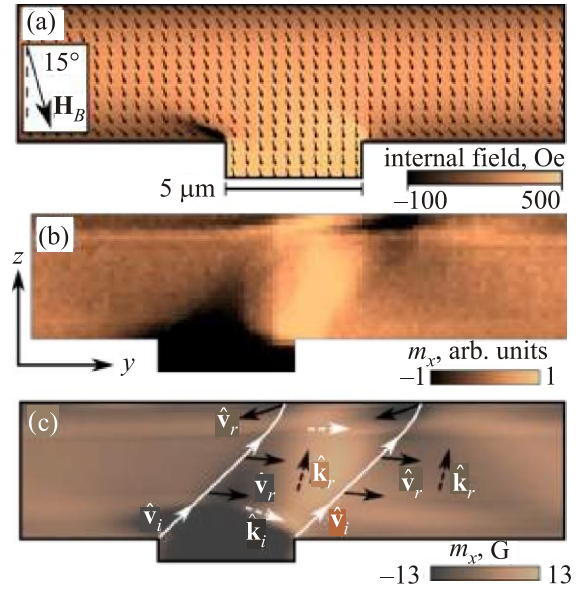

Fig. 4. (Color online) Spin waves in an asymmetrically magnetized Permalloy *T*-junction (after Ref. 10). (a) The calculated distributions of the static magnetisation (arrows) and the projection of the internal magnetic field onto the magnetization (color scale) are shown for the magnetic field of $H_B = 500$ Oe applied at 15° to the vertical symmetry axis. Each arrow represents the average of 5×5 mesh cells. (b) A TRSKM snapshot of the spin-wave beam propagating into the arm of the Permalloy *T*-junction is shown for the bias magnetic field of $H_B = 500$ Oe applied at 15° relative to the leg of the junction. The frequency of the cw magnetic "pump" field was 8.24 GHz. (c) The numerically simulated out-of-plane component of the dynamic magnetization corresponding to the experimental snapshot from panel (b) is shown together with the directional unit vectors of the group velocities $\hat{\mathbf{v}}$ and wave vectors $\hat{\mathbf{k}}$ extracted for the incident (index "*i*") and reflected (index "*r*") spin-wave beams at $k_x = 0.94$ µm^{-1}. The pumping frequency in the simulations was 7.52 GHz. The difference in the frequency values in the experiments and simulations was due to inevitable differences between the measured and simulated samples.

magnetization and the wave vector, or to curvature of the static magnetization. In the former case, the graded magnonic index can lead to scattering and even transformation of the propagating spin wave [47,48]. In the latter case, the curved magnetization can lead to such exotic effects as the curvature induced ("geometrical") magnetic anisotropy [49,50], which could be described in terms of magnetic energy contributions characteristic of the Dzyaloshinskii–Moriya interaction [51,52].

At the same time, transverse Bloch-type magnetic domain walls represent a natural reflectionless potential for propagating spin waves. Indeed, spin waves propagating through such domain walls preserve their amplitude but acquire a phase shift. This phase shift is directly related to

the magnetization rotation within the domain wall - specifically, the spin-wave phase shifts are 90° and 180° for 180° and 360° domain walls, respectively. In contrast to Bloch walls, the amplitude reflectivity of spin waves from Néel-type magnetic domain walls can vary significantly (ranging between the extremes of zero and unity) depending on the thickness of the film and the wave vector. Given that magnetic domain walls themselves have been proposed as information carriers, there is also scope for creating hybrid spin-wave/domain-wall devices.

In addition to the interaction of plane spin waves with confined regions of graded magnonic index, a traditionally active and discovery-rich research area of magnonics has dealt with spin waves in extended, strongly nonuniform micromagnetic states and textures, featuring magnetic vortices and antivortices [56–59], complex domain structures and skyrmions [62,63]. The relevant research results are reviewed in other articles of this Special Issue [64–66].

At last but not least, the graded magnonic index can and has in fact been used in design of magnonic crystals [67] in several ways. The nonuniform internal magnetic field can either serve to modulate the magnonic properties in the direction of spin wave propagation [68,69], or to channel spin waves through e.g. topographically defined landscapes [70,71]. Alternatively, as discussed earlier, the same can be achieved as a result of the non-uniform configuration of the magnetization in patterned magnetic films [72–74].

4. Conclusions and outlook

Over the past decade, magnonics has emerged as one of the most rapidly growing research fields in magnetism and a potential rival of semiconductor technology in the field of data communication and processing. However, together with loss reduction, the control of the spin-wave trajectory, the shortening of the wavelength of studied spin waves and the associated miniaturization of realized functional magnonic devices remain major challenges in both experimental research and technological development in magnonics. Here, we have reviewed the concept of graded-index magnonics, which could help meet these challenges. Indeed, the propagation of spin waves in graded magnonic media can be controlled using sub-wavelength, continuously varying magnetic non-uniformities rather than physical patterning. This should minimize scaling of the magnonic device size with the spin-wave wavelength, in contrast to e.g. magnonic crystal based approaches. This sort of crossover from studying magnonic phenomena associated with ubiquitous nonuniformity of micromagnetic configurations in geometrically patterned magnetic systems to the exploitation of the graded magnonic index is predicted to drive the magnonics research in the nearest future.

From the point of view of the Landau–Lifshitz equation, this trend will lead to two major directions of theoretical development. Within the first of them, the concepts, ideas and sometimes whole classes of solutions and theoretical methods developed in transformation optics and quantum mechanics will continue to be mapped onto magnonic systems [42,49,50]. In particular, the study of exchange spin waves, which have an isotropic dispersion described by a parabolic law in the continuous medium approximation, will benefit from this approach. Within the second direction, researchers will face the challenge of developing a completely new theoretical formalism that will fully account for the rich and exciting complexities inherent to the Landau–Lifshitz equation. In addition to the already discussed anisotropic dispersion of magnetostatic and dipole-exchange spin waves, the challenges include the non-linearity of the Landau–Lifshitz equation [75,76] and exotic contributions to the magnetic energy, such as the magneto-elastic coupling [77,78] and (nonreciprocal) Dzyaloshinskii–Moriya [51,52] interaction, and magnetic dissipative function [79,80].

We have limited the discussion above to the case of patterned thin-film magnetic structures, which are in the focus of current experimental studies and in which the graded magnonic index is created by virtue of their patterning. The key advantage of such samples is that, due to the magnetic hysteresis, their graded magnonic landscapes could potentially be programmed e.g. by the external magnetic field [81]. However, it is clear that the scope of the concept is far broader. Indeed, the graded magnonic index can be created through application of external non-uniform stimuli, ranging from the magnetic field due to the electrical currents [82] or magnetic charges [83] through to electric field, spin currents [85] and thermal gradients, including those created optically [25,87,88]. An exciting extension of the concept is that of non-stationary, dynamically controlled graded-index landscapes [89,90]. Alternatively, the means of nano- and micro-scale materials engineering allow one to create essentially arbitrary magnonic landscapes [91–94], provided that the spin-wave damping could be controlled at a reasonably low level. Finally, one should not forget that the world of magnetic materials is not limited to transition metal ferromagnet and YIG samples. Indeed, the spin dynamics and therefore spin waves in multi-sublattice magnetic materials are generally faster and arguably richer than one might think [95,97], and are still governed by the generalization of the Landau–Lifshitz equation. Extension of the graded-index magnonics concept to such systems is certainly possible but is beyond the scope of this paper.

The range of spin-wave phenomena covered by this brief review challenges both the expertise of the authors and the journal page limits for this Special Issue. Yet, we hope that our contribution will help to inspire and guide future researchers though the exciting world of graded-index magnonics, which is both governed and created by the Landau–Lifshitz equation.

1. V.V. Kruglyak, S.O. Demokritov, and D. Grundler, *J. Phys. D* **43**, 264001 (2010), and references therein.

2. A.I. Akhiezer, V.G. Bar'yakhtar, and S.V. Peletminskii, *Spin Waves*, North-Holland, Amsterdam (1968).

3. A.G. Gurevich and G.A. Melkov, *Magnetization Oscillations and Waves*, Chemical Rubber Corp., New York (1996).

4. L. D. Landau and E. Lifshitz, *Phys. Z. Sow.* **8**, 153 (1935).

5. A.V. Vashkovskii, A.V. Stalmakhov, and D.G. Shakhnazaryan, *Izv. Vys. Uch. Zav. Fizika* **31**, 67 (1988).

6. A.V. Vashkovskii and V.I. Zubkov, *J. Commun. Technol. Electron.* **48**, 131 (2003).

7. A.V. Vashkovskii and E.G. Lokk, *Phys. Usp.* **47**, 601 (2004).

8. S.-K. Kim, S. Choi, K.-S. Lee, D.-S. Han, D.-E. Jung, and Y.-S. Choi, *Appl. Phys. Lett.* **92**, 212501 (2008).

9. T. Schneider, A.A. Serga, A.V. Chumak, C.W. Sandweg, S. Trudel, S. Wolff, M.P. Kostylev, V.S. Tiberkevich, A.N. Slavin, and B. Hillebrands, *Phys. Rev. Lett.* **104**, 197203 (2010).

10. C.S. Davies et al. (unpublished).

11. E.W. Marchand, *Gradient Index Optics*, Academic Press, London (1978).

12. J. B. Pendry, A.I. Fernandez-Dominguez, Y. Luo, and R. Zhao, *Nat. Phys.* **9**, 518 (2013).

13. *International Technology Roadmap for Semiconductors* (ITRS), *Emerging Research Devices* (2013); http://www.itrs.net/Links/2013ITRS/Summary2013.htm (accessed 31 January 2015).

14. Y.I. Gorobets and S.A. Reshetnyak, *Techn. Phys.* **43**, 188 (1998).

15. Y.I. Gorobets and S.O. Reshetnyak, *Met. Nov. Tekhnol.* **25**, 1099 (2003).

16. E.H. Lock, *Phys. Usp.* **51**, 375 (2008).

17. S.-K. Kim, *J. Phys. D* **43**, 264004 (2010), and references therein.

18. M. Dvornik, Y. Au, and V.V. Kruglyak, *Top. Appl. Phys.* **125**, 101 (2013), and references therein.

19. M. Donahue and D. Porter, *Inter. Rep. NISTIR 6376*, NIST, Gaithersburg, MD (1999).

20. R.W. Damon and J.R. Eshbach, *J. Phys. Chem. Solids* **19**, 308 (1961).

21. A.V. Vashkovsky and E.H. Lock, *Phys. Usp.* **49**, 389 (2006), and references therein.

22. B.A. Kalinikos and A.N. Slavin, *J. Phys. C* **19**, 7013 (1986).

23. The Permalloy samples considered here were assumed to have $M_S = 860$ G and $A = 1.3$ μerg/cm.

24. V. Veerakumar and R.E. Camley, *Phys. Rev. B* **74**, 214401 (2006).

25. Y. Au, M. Dvornik, T. Davison, E. Ahmad, P.S. Keatley, A. Vansteenkiste, B. Van Waeyenberge, and V.V. Kruglyak, *Phys. Rev. Lett.* **110**, 097201 (2013).

26. R. Gieniusz, H. Ulrichs, V.D. Bessonov, U. Guzowska, A.I. Stognii, and A. Maziewski, *Appl. Phys. Lett.* **102**, 102409 (2013).

27. K.-S. Lee and S.-K. Kim, *J. Appl. Phys.* **104**, 053909 (2008).

28. A. Khitun, M. Bao, and K.L. Wang, *J. Phys. D* **43**, 264005 (2010).

29. S.S. Mukherjee, J.H. Kwon, M. Jamali, M. Hayashi, and H. Yang, *Phys. Rev. B* **85**, 224408 (2012).

30. D.-E. Jeong, D.-S. Han, S. Choi, and S.-K. Kim, http://arxiv.org/ftp/arxiv/papers/0901/0901.1700.pdf.

31. J. Jorzick, S.O. Demokritov, B. Hillebrands, M. Bailleul, C. Fermon, K.Y. Guslienko, A.N. Slavin, D.V. Berkov, and N.L. Gorn, *Phys. Rev. Lett.* **88**, 47204 (2002).

32. J.P. Park, P. Eames, D.M. Engebretson, J. Berezovsky, and P.A. Crowell, *Phys. Rev. Lett.* **89**, 277201 (2002).

33. V.V. Kruglyak, A. Barman, R.J. Hicken, J.R. Childress, and J.A. Katine, *Phys. Rev. B* **71**, 220409 (2005).

34. M. Dvornik, P.V. Bondarenko, B.A. Ivanov, and V.V. Kruglyak, *J. Appl. Phys.* **109**, 07B912 (2011).

35. V.E. Demidov, S.O. Demokritov, K. Rott, P. Krzysteczko, and G. Reiss, *Appl. Phys. Lett.* **92**, 232503 (2008).

36. X.J. Xing, S.W. Li, X.H. Huang, and Z.G. Wang, *AIP Adv.* **3**, 032144 (2013).

37. M. Krawczyk, *J. Phys. Conf. Ser.* **200**, 072056 (2010).

38. V.E. Demidov, J. Jersch, S.O. Demokritov, K.Rott, and P. Krzysteczko, G. Reiss, *Phys. Rev. B* **79**, 054417 (2009).

39. C. Bayer, J.P. Park, H. Wang, M. Yan, C.E. Campbell, and P.A. Crowell, *Phys. Rev. B* **69**, 134401 (2004).

40. G. Duerr, K. Thurner, J. Topp, R. Huber, and D. Grundler, *Phys. Rev. Lett.* **108**, 227202 (2012).

41. V.E. Demidov, M.P. Kostylev, K. Rott, J. Münchenberger, G. Reiss, and S.O. Demokritov, *Appl. Phys. Lett.* **99**, 082507 (2011).

42. E. Schlömann, *J. Appl. Phys.* **35**, 159 (1964).

43. Y. Au, T. Davison, E. Ahmed, P.S. Keatley, R.J. Hicken, and V.V. Kruglyak, *Appl. Phys. Lett.* **98**, 122506 (2011).

44. M. Arikan, Y. Au, G. Vasile, S. Ingvarsson, V.V. Kruglyak, *J. Phys. D* **46**, 135003 (2013).

45. P. Gruszecki, J. Romero-Vivas, Y.S. Dadoenkova, N.N. Dadoenkova, I.L. Lyubchanskii, and M. Krawczyk, *Appl. Phys. Lett.* **105**, 242406 (2014).

46. G. Duerr, R. Huber, and D. Grundler, *J. Phys.: Condens. Matter* **24**, 024218 (2012), and references therein.

47. X. Xing, W. Yin, and Z. Wang, *J. Phys. D* **48**, 215004 (2015).

48. A.V. Sadovnikov, C.S. Davies, S.V. Grishin, V.V. Kruglyak, D.V. Romanenko, Y.P. Sharaevskii, and S.A. Nikitov, *Appl. Phys. Lett.* (submitted).

49. V.S. Tkachenko, A.N. Kuchko, M. Dvornik, and V.V. Kruglyak, *Appl. Phys. Lett.* **101**, 152402 (2012).

50. V.S. Tkachenko, A.N. Kuchko, and V.V. Kruglyak, *Fiz. Nizk. Temp.* **39**, 214 (2013) [*Low Temp. Phys.* **39**, 163 (2013)].

51. I. Dzyaloshinsky, *J. Phys. Chem. Solids.* **4**, 241 (1958).

52. D.D. Sheka, V.P. Kravchuk, and Y. Gaididei, *J. Phys. A* **48**, 125202 (2015).

53. R. Hertel, W. Wulfhekel, and J. Kirschner, *Phys. Rev. Lett.* **93**, 257202 (2004).

54. C. Bayer, H. Schultheiss, B. Hillebrands, and R. Stamps, *IEEE Trans. Magn.* **41**, 3094 (2005).

55. S. Macke and D. Goll, *J. Phys.: Conf. Ser.* **200**, 042015 (2010).

56. K.Y. Guslienko, B.A. Ivanov, V. Novosad, Y. Otani, H. Shima, and K. Fukamichi, *J. Appl. Phys.* **91**, 8037 (2002).

57. B.A. Ivanov and C.E. Zaspel, *J. Appl. Phys.* **95**, 7444 (2004).

58. C. Ragusa, M. Carpentieri, F. Celegato, P. Tiberto, E. Enrico, L. Boarino, and G. Finocchio, *IEEE Trans. Magn.* **47**, 2498 (2011).

59. K.Y. Guslienko, G.N. Kakazei, Y.V. Kobljanskyj, G.A. Melkov, V. Novosad, and A.N. Slavin, *New J. Phys.* **16**, 063044 (2014).

60. C. Patschureck, K. Lenz, M.O. Liedke, M.U. Lutz, T. Strache, I. Mönch, R. Schäfer, L. Schultz, and J. McCord, *Phys. Rev. B* **86**, 054426 (2012).

61. C. Hamann, R. Mattheis, I. Mönch, J. Fassbender, L. Schultz, and J. McCord, *New J. Phys.* **16**, 023010 (2014).

62. C. Schütte and M. Garst, *Phys. Rev. B* **90**, 094423 (2014).

63. M. Mochizuki, X.Z. Yu, S. Seki, N. Kanazawa, W. Koshibae, J. Zang, M. Mostovoy, Y. Tokura, and N. Nagaosa, *Nat. Mater.* **13**, 241 (2014).

64. C.E. Zaspel and V.E. Kireev, *Fiz. Nizk. Temp.* **41**, No. 10 (2015) [*Low Temp. Phys.* **41**, No. 10 (2015)].

65. G.M. Wysin, *Fiz. Nizk. Temp.* **41**, No. 10 (2015) [*Low Temp. Phys.* **41**, No. 10 (2015)].

66. S. Schroeter and M. Garst, *Fiz. Nizk. Temp.* **41**, No. 10 (2015) [*Low Temp. Phys.* **41**, No. 10 (2015)].

67. S.A. Nikitov, P. Tailhades, and C.S. Tsai, *J. Magn. Magn. Mater.* **236**, 320 (2001).

68. S. Neusser, B. Botters, and D. Grundler, *Phys. Rev. B* **78**, 054406 (2008).

69. S. Tacchi, B. Botters, M. Madami, J.W. Klos, M.L. Sokolovskyy, M. Krawczyk, G. Gubbiotti, G. Carlotti, A.O. Adeyeye, S. Neusser, and D. Grundler, *Phys. Rev. B* **86**, 014417 (2012).

70. T. Schwarze and D. Grundler, *Appl. Phys. Lett.* **102**, 222412 (2013).

71. M. Krawczyk, S. Mamica, M. Mruczkiewicz, J.W. Klos, S. Tacchi, M. Madami, G. Gubbiotti, G. Duerr, and D. Grundler, *J. Phys. D* **46**, 495003 (2013).

72. A.Y. Galkin, B.A. Ivanov, and C.E. Zaspel, *Phys. Rev. B* **74**, 144419 (2006).

73. A.A. Awad, G.R. Aranda, D. Dieleman, K.Y. Guslienko, G.N. Kakazei, B.A. Ivanov, and F.G. Aliev, *Appl. Phys. Lett.* **97**, 132501 (2010).

74. X.-G. Wang, G.-H. Guo, Z.-X. Li, D.-W. Wang, Y.-Z. Nie, and W. Tang, *Eur. Phys. Lett.* **109**, 37008 (2015).

75. A.M. Kosevich, B.A. Ivanov, and A.S. Kovalev, *Phys. Rep.* **194**, 117 (1990), and references therein.

76. R.K. Dumas, E. Iacocca, S. Bonetti, S.R. Sani, S.M. Mohseni, A. Eklund, J. Persson, O. Heinonen, and J. Akerman, *Phys. Rev. Lett.* **110**, 257202 (2013).

77. S. Nikitov, Y. Filimonov, S. Vysotsky, Y. Khivintsev, E. Pavlov, *2012 IEEE Int. Ultrasonics Symp. Proc.* 1240 (2012).

78. O. Prikhod'ko, O.S. Sukhorukova, S.V. Tarasenko, and V.G. Shavrov, *JETP Lett.* **100**, 319 (2014).

79. V.G. Bar'yakhtar, B.A. Ivanov, T.K. Soboleva, and A.L. Sukstanskii, *Zh. Eksp. Teor. Fiz.* **64**, 857 (1986).

80. V.G. Baryakhtar and A.G. Danilevich, *Fiz. Nizk. Temp.* **39**, 1279 (2013) [*Low Temp. Phys.* **39**, 993 (2013)], and references therein.

81. M. Krawczyk and D. Grundler, *J. Phys.: Condens. Matter* **26**, 123202 (2014), and references therein.

82. S.O. Demokritov, A.A. Serga, A. Andre, V.E. Demidov, M.P. Kostylev, B. Hillebrands, and A.N. Slavin, *Phys. Rev. Lett.* **93**, 047201 (2004).

83. H.-J. Chia, F. Guo, L.M. Belova, and R.D. McMichael, *Phys. Rev. Lett.* **108**, 087206 (2012).

84. A.B. Ustinov and B.A. Kalinikos, *Tech. Phys. Lett.* **40**, 568 (2014).

85. V.E. Demidov, S. Urazhdin, A.B. Rinkevich, G. Reiss, and S.O. Demokritov, *Appl. Phys. Lett.* **104**, 152402 (2014).

86. G.E.W. Bauer, E. Saitoh, and B.J. van Wees, *Nat. Mater.* **11**, 391 (2012).

87. T. Satoh, Y. Terui, R. Moriya, B.A. Ivanov, K. Ando, E. Saitoh, T. Shimura, and K. Kuroda, *Nat. Photon.* **6**, 662 (2012).

88. O. Kolokoltsev, N. Qureshi, E. Mejia-Uriarte, and C.L. Ordonez-Romero, *J. Appl. Phys.* **112**, 013902 (2012).

89. A.V. Chumak, A.D. Karenowska, A.A. Serga, and B. Hillebrands, *Top. Appl. Phys.* **125**, 243 (2013), and references therein.

90. A.A. Nikitin, A.B. Ustinov, A.A. Semenov, A. V. Chumak, A.A. Serga, V.I. Vasyuchka, E. Lahderanta, B.A. Kalinikos, and B. Hillebrands, *Appl. Phys. Lett.* **106**, 102405 (2015).

91. A.M. Kuchko, *Metall. Nov. Tekhnol.* **27,** 511 (2005).

92. S.V. Vasiliev, V.V. Kruglyak, M.L. Sokolovskii, and A.N. Kuchko, *J. Appl. Phys.* **101**, 113919 (2007).

93. P. Gawronski, K.J. Merazzo, O. Chubykalo-Fesenko, R.P. del Real, and M. Vazquez, *Nanotechnology* **25**, 475703 (2014).

94. V.E. Demidov, S. Urazhdin, A. Zholud, A.V. Sadovnikov, and S.O. Demokritov, *Appl. Phys. Lett.* **106**, 022403 (2015).

95. B.A. Ivanov, *Fiz. Nizk. Temp.* **31**, 841 (2005) [*Low Temp. Phys.* **31**, 635 (2005)], and references therein.

96. L.J. Heyderman and R.L. Stamps, *J. Phys. Condens. Matter* **36**, 363201 (2014), and references therein.

97. B.A. Ivanov, *Fiz. Nizk. Temp.* **40**, 119 (2014) [*Low Temp. Phys.* **40**, 91 (2014)], and references therein.